Electromechanical Modelling and Control of a Micro-Wind Generation System for Isolated Low Power DC Micro Grids

Alba Colet-Subirachs[1,2], Oriol Gomis-Bellmunt[1,2], Daniel Clos-Costa[3], Guillermo Martín-Segura[1], Adrià Junyent-Ferre[1], Roberto Villafáfila-Robles[1], Laia Ferrer-Marti[3]

[1] Centre d'Innovació Tecnològica en Convertidors Estàtics i Accionaments (CITCEA-UPC), Departament d'Enginyeria Elèctrica, Universitat Politècnica de Catalunya, ETS d'Enginyeria Industrial de Barcelona, Barcelona, Spain
[2] IREC Catalonia Institute for Energy Research, Josep Pla, Barcelona, Spain
[3] Grup de Recerca en Cooperació i Desenvolupament Humà (GRECDH), Departament d'Enginyeria Mecànica, Universitat Politècnica de Catalunya, ETS d'Enginyeria Industrial de Barcelona, Barcelona, Spain

Keywords: «Wind turbine», «Wind energy», «Synchronous generator».

Abstract

This paper describes the modelling and control of a micro-wind generation system, based on an axial flux permanent magnet synchronous generator (PMSG), for isolated low power DC micro grids. The system consists of a micro-wind turbine including a furling tail, a PMSG, a three phase diode rectifier and a buck converter connected to a battery bank and a load. Furthermore, it incorporates a control system to extract the maximum power output from the wind turbine using the minimum possible number of sensors. The system is simulated in Matlab/Simulink to analyze the dynamical response and it is compared with the current IT-PE-100.

Introduction

In recent years, many power converter techniques have been developed for integrating wind turbine generation systems in the electrical grid [1, 2, 3, 4]. However, there are not many works focused on 'Micro Wind Turbines', especially for those up to 1 kW. These kinds of turbines are currently used [5] in stand-alone systems and to feed isolated and small communities like country villages or rural schools[6]. Batteries are widely used in stand-alone small wind turbine generator systems to store the energy surplus and supply the load in case of low renewable energy production [7]. Nevertheless, the systems efficiency depends on many factors such as the converter topology and the controller. These configurations have been studied in [8, 9, 10, 11].

The present paper deals with the modelling of the entire electromechanical system of a micro-wind turbine including a controller to extract the maximum power available from the wind. The model is addressed by considering the turbine components, identified experimentally and using data provided by MSC Adams aerodynamic and mechanical simulation. Simulations are performed using Matlab/Simulink, including simplified mechanical models and detailed electrical and control parts.

System description

The wind turbine generation system studied, IT-PE-100 developed by ITDG-Practical Action (Fig. 1), [12, 13] consists basically in a fixed-pitch three-bladed, horizontal axis micro-wind turbine coupled through a direct transmission to an axial flux permanent magnet synchronous generator [14]. A three phase diode bridge rectifier and a battery charger are used to charge a battery bank.

In order to achieve the maximum power tracking and output voltage regulation within a wide range of wind speed variation, it is proposed a configuration which includes a dc–dc buck converter,

Fig. 1: Photographs of the IT-PE-100 wind turbine generation system (Communities of Campo Alegre and El Alumbre in Cajamarca, Peru, 2007)

a three-phase rectifier and a battery bank (Fig. 2). This configuration avoids the use of mechanical sensors to not increase the installation and maintenance cost. For this reason, it provides a simple and economical stand-alone wind energy system.

The system has two controllers of different nature:

– the passive mechanical control, which limits the maximum power obtained from the wind by using a passive controlled yaw mechanism based on a non aligned wind turbine rotor and a free furling tail;
– the electrical control, which handles to feed the batteries with an appropriate constant dc voltage regulating the duty cycle of the buck converter; the converter is capable of increasing or decreasing the input voltage (rectifier output side); hence, increased energy capture will be possible both at the high and the low end of the speed range.

The two control systems interact so that at low wind speeds the electrical control system maximizes the power captured from the

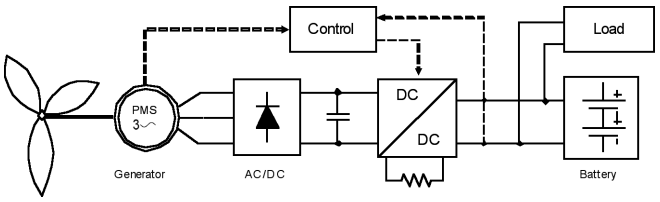

Fig. 2: Schematic diagram of the stand-alone wind energy system under consideration.

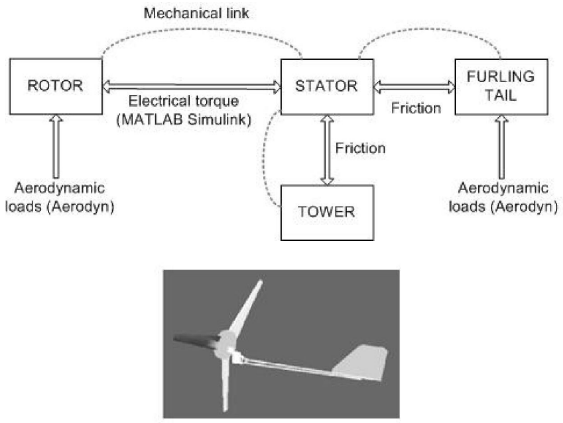

Fig. 3: MSC. Adams system block description

turbine while at high wind speeds the mechanical control system allows the rotor to furl (turn away from the wind direction) decreasing the power captured.

Modelling

The system simulations have been carried out using Matlab/Simulink®. To study the dynamical response in Matlab, the system model has been separated in different functional subsystems: the wind turbine, the transmission and the control block are implemented using equation model blocks while the electrical subsystem uses the SimPowerSystemsTM library.

A mechanical simulation including the furling tail and friction forces has been done using the MSC.Adams software linked with NTWC AeroDyn software library [15]. An example model block is shown in Fig. 3.

This simulation has allowed to obtain the turbine characteristic parameters, specifically: the curves shown in Fig. 4 and the turbine inertia.

Mechanical subsystem

The mechanical subsystem contains the equations that approximate the behaviour of the wind turbine and the transmission:

The Simulink model of turbine takes as input the wind speed v_w, the rotational speed of the turbine ω_t and gives as output the turbine torque, Γ_t. The mechanical power developed by a wind turbine rotor varies according to the equation:

$$P_t = \frac{1}{2} C_p \, \rho \, \pi \, r^2 v_w^3 \tag{1}$$

And the torque:

$$\Gamma_t = \frac{1}{2} \frac{C_p \, \rho \, \pi \, r^2 v_w^{\,3}}{\omega_t} \tag{2}$$

Where: C_p Turbine coefficient of performance
ρ Air density
r Radius of the blade
v_w Wind speed

The power curve of the IT-PE-100 turbine, which links the power turbine coefficient with the tip speed ratio, $\lambda = \frac{r \cdot \omega_t}{v_w}$, has been implemented as a table of values, given by the response simulations developed in MSC Adams. The curve under consideration is shown in Fig. 4, where φ is the turn angle of the turbine rotor against the wind flow.

In order to simplify the study, the case taken into consideration for electrical and control purposes is when $\varphi = 0°$. This curve corresponds to the orientation of the rotor turbine that captures the maximum power, i.e. when the rotor is perpendicular to the wind flow.

The transmission block implements the system described by the differential equation (3). The model takes as input torque of the turbine and the engine torque and gives as output the rotation speed of the shaft coupling between the turbine and motor.

$$\frac{1}{J}\left(\Gamma_t - \Gamma_m\right) = \frac{\mathrm{d}}{\mathrm{d}t}\omega_t \tag{3}$$

Where: Γ_w Generator torque
J Turbine inertia

Electrical subsystem

The electric circuit model of Simulink® implements the equations of an axial flux permanent magnet synchronous machine (AFPMSG), the rectifier, the buck converter and the battery. These media have been implemented using SimPowerSystems$_{TM}$. The model takes as input the rotational speed of the turbine and a digital signal from the control system, which controls the duty cycle of the buck converter. The outputs are the stator voltages, the converter output voltage and the generator torque. The electric circuit implemented is shown in Fig. 5.

The permanent magnet synchronous generator has been modelled as an AC voltage source in series with an inductor and a resistor. The amplitude and frequency of this source depends on the rota-

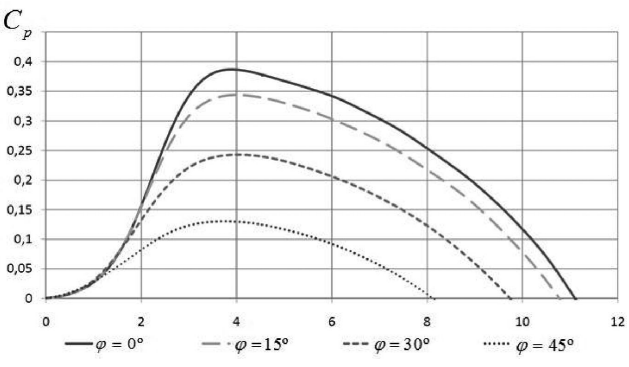

Fig. 4: Relation between C_p and λ for a different wind turbine φ in the IT-PE-100.

tional speed of the rotor:

$$E_s = K \cdot p \cdot \omega_t \tag{4}$$

$$f_r = p \cdot \frac{\omega_t}{2\pi} \tag{5}$$

Where: E_s Per-phase generated emf voltage
K Constant derived from the alternator
F_r Electrical frequency
p Pair of poles

Inductance L_s, and resistance, R_s, are respectively the inductance and internal resistance of the generator. The electromechanical torque can be expressed as a function of the armature currents:

$$\Gamma_m = K_t I_s \tag{6}$$

Where: K_t Peak per phase torque constant
I_s Stator current

The rectifier is an uncontrolled diode bridge composed of six diodes. The buck converter consists of a power MOSFET as a switch, a diode, an inductor and a filter capacitor. The function of the converter is to vary the DC voltage on its input side (which is the rectifier output voltage) according a signal provided by a controller. The battery bank may be represented as a voltage source connected in series with a resistance. This model is a simplified version of a more detailed model of lead-acid batteries reported in [16].

Control subsystem

This subsystem, shown in Fig. 6, is a sensorless power tracker. It is divided in two blocks: the control converter block, which obtains the DC desired voltage from the rotational speed and the PLL to compute the rotational wind turbine speed from the three-phase generator output voltages.

The control block implements the regulation of the bus voltage using two inputs, the reference value of input voltage to the converter, v_{dc}, which is calculated with an expression as a function of the turbine rotational speed, and the constant voltage on the edge of the converter fixed by the battery, v_{bat}. The output is a digital PWM signal to control the MOSFET of the buck converter.

The PLL block contains the Park matrix and a proportional-integral controller (PI) to get the speed of the three-phase input voltages. These input voltages are the terminal voltages of the generator. The block output is the rotational speed of the turbine.

Control algorithm

The objective is to work at the optimum tip-speed ratio, that is, when the turbine produces the maximum power. In this case the mechanical torque developed by the turbine is still a function proportional to the square of the speed.

$$\Gamma_{t,opt} = K_{opt} \omega_2 \tag{7}$$

Where:

$$K_{opt} = \frac{1}{2} \frac{\rho \, \pi \, r^5 \, C_{P,max}}{\lambda_{opt}^3}$$

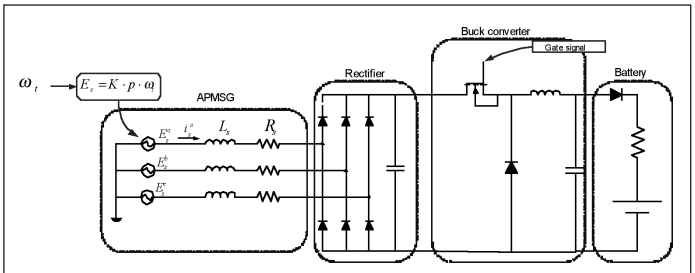

Fig. 5: Electrical circuit subsystem implemented in SimPowerSystems™

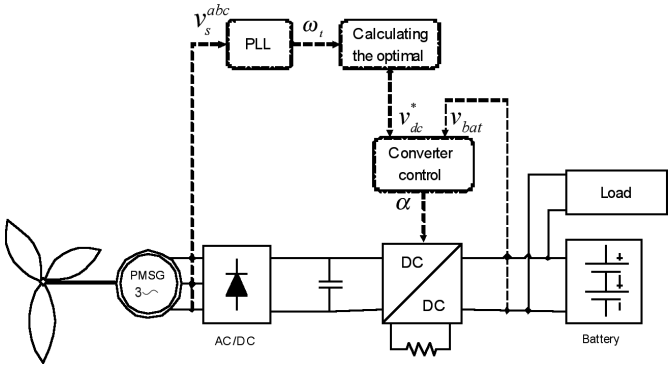

Fig. 6: chematic diagram of the electrical system control under consideration

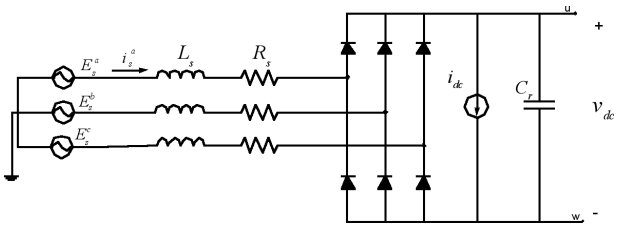

Fig. 7: Electrical circuit of a three-phase rectifier with a non ideal source

Γ_{topt} target torque developed by de turbine
$C_{p,max}$ maximum power-coefficient
φ_{opt} target tip-speed ratio

A common way to accomplish this goal is to use the known constant tip speed ratio control. In steady state the rotational speed of the shaft coupling is constant. Thus, the dynamic equation that modelled the transmission system (3) is balanced pairs: $\Gamma_t - \Gamma_m = 0$. From which it is possible to relate the optimal parameters of turbine with the generator variables and obtain an expression of the optimal stator current as a function of the characteristic system parameters. Rearranging (6) and (7):

$$I_{s,opt} = \frac{K_{opt}}{K_t} \omega^2 \tag{8}$$

Considering the circuit modelled in Fig. 7, an approximation of the rectifier dc-link voltage may be obtained using the standard equations of a three phase full bridge diode rectifier with line inductance in series with a resistance [17, 18].

$$v_{dc} = \frac{3}{\pi}\sqrt{6} \cdot E_s(\omega_t) - \frac{3}{\pi} R_s \cdot I_s(\omega_t) - \frac{3}{\sqrt{6}} \omega_r \cdot L_s \cdot I_s(\omega_t) \tag{9}$$

Replacing in (9) the induced voltage (3) and stator current by the characteristic parameters of the generator and the turbine parameters at the optimum (8), it is possible to express the optimal rectifier output voltage based on the rotational speed:

$$v_{dc}^{*} = \left(\frac{3}{\pi}\sqrt{6}K \cdot p\right)\cdot\omega_t - \left(\frac{3}{\pi}R_s\frac{K_{opt}}{K_t}\right)\cdot\omega_t^2 - \left(\frac{3}{\sqrt{6}}L_s \cdot p \cdot \frac{K_{opt}}{K_t}\right)\cdot\omega_t^3 \quad (10)$$

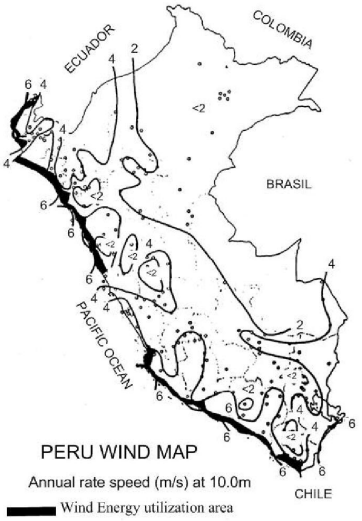

Fig. 8: Peru wind map at an altitude 10m over the ground [18]

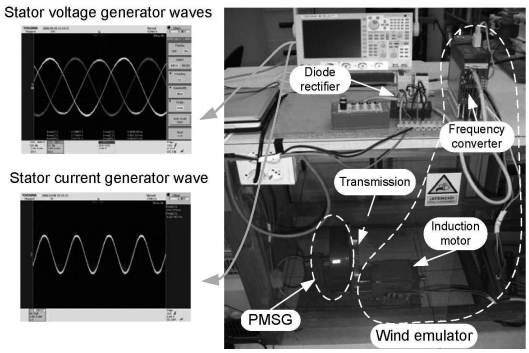

Fig. 9: Test platform and voltage and current waveforms

Table 1: System parameters

Parameter	Symbol	Value	Units
Effective turbine radius	r	0,85	m
Air density	ρ	1,23	kg/m^3
Maximum wind turbine power coefficient	$C_{p,max}$	0,3865	
Optimum tip speed ratio	λ_{opt}	3,8810	
System inertia	J	0,785	kg/m^2
Battery nominal voltage	v_{bat}	12	V
Pair of poles	P	4	
Phase winding resistance	R_s	0,35	Ω
Phase winding inductance	L_s	0,01	H
Rotor flux constant	K	0,0927	V_{rms}/rad·s^{-1}

As a result, the duty cycle of the converter, which is the output control subsystem signal, is:

$$\alpha^{*} = \frac{v_{bat}}{v_{dc}^{*}} \quad (11)$$

v_{bat} terminal battery voltage.

Simulation study

In order to evaluate the dynamic performance of the system and the control operation, an example using a wind-speed variation was developed. The range of wind speed values was chosen taking into account the average wind speed in the area with the highest wind potential in Peru, where the studied wind turbines are located [19]. This is placed on the coast and in some areas of the sierra (Fig. 8) and takes the average wind of 6 m/s at an altitude of 10 m.

The wind speed function is introduced as a step series from 5 m/s to 6,5m/s. Each wind step is maintained during an interval of 20s. The simulation starts at the t = 30s, where the system is in steady state, and finishes at t = 110s.

The wind turbine system parameters used in the simulation are shown in Tab. 1. These parameters were obtained from the IT-PE-100 data manuals and the test performed by using the test platform shown in Fig. 9. In this test platform, wind is emulated with an induction motor controlled by a frequency converter. The emulator is mechanically attached to the PMSG.

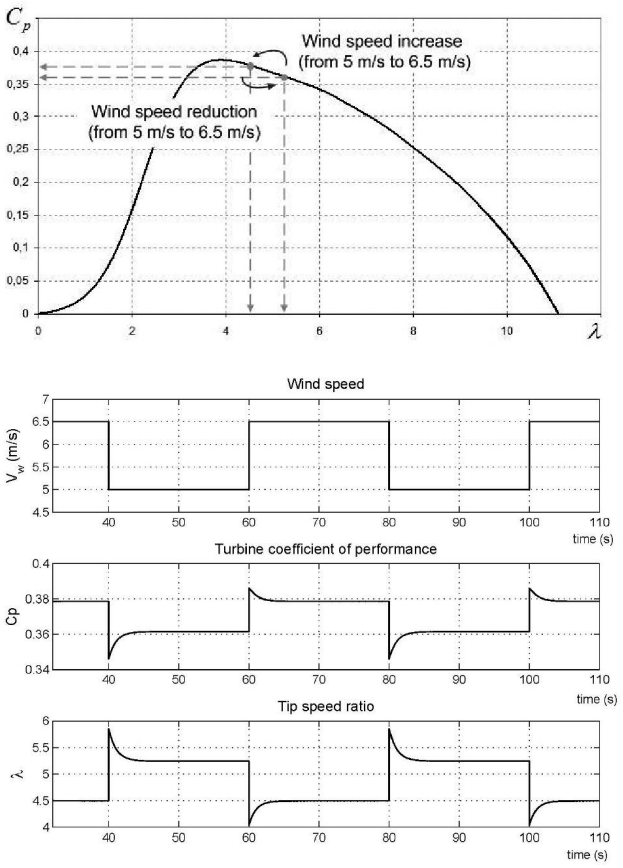

Fig. 10: System operation point in the C_p – λ curve and time variable response for a wind step input

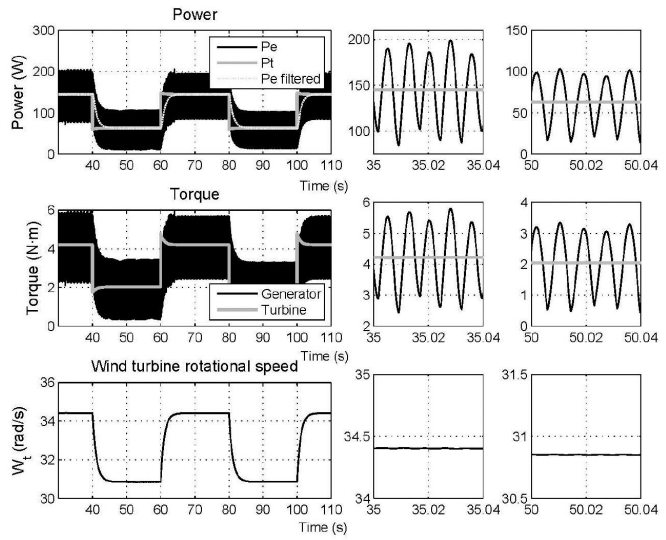

Fig. 11: Time variable response of power, torque and rotational for a wind step input

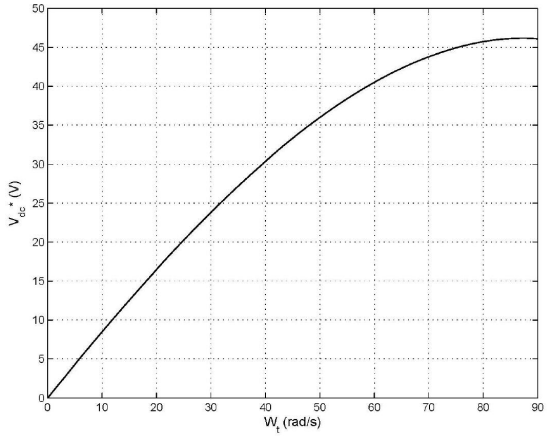

Fig. 12: Ideal relationship between the optimal dc voltage and the rotational turbine speed

Figs. 10-14 present the results obtained using Matlab-Simulink™. A sudden increase in wind speed causes a transition in that the value decreases and the λ value increases (Fig. 10) until the system stabilizes in an equilibrium point (C_p = 0,3786, λ = 4, 498) near the λ_{opt} which corresponds to the $C_{p,max}$.

The wind gust causes an increase in the torque transmitted from the turbine to the generator (Fig. 11). The turbine in response will try to accelerate. As a consequence, the power increases.

The turbine acceleration results in an increase on the generator electrical frequency, which in turn causes an increase in the v^*_{dc} desired voltage of the control system (Fig. 12).

Moreover, considering the case in what the wind speed falls from 6,5 m/s to 5 m/s, λ increase and C_p decrease (Fig. 10) until a new equilibrium point (C_p = 0,3614 λ = 5, 246). The turbine torque will fall and the inductance and inertia will act as a braking device for slowing the rotational speed (Fig. 11).

This speed reduction will decrease the electrical frequency which in turn will reduce the dc bus voltage.

Comparing the performance of the controlled and uncontrolled current system (IT-PE-100 wind turbine model) another simula-

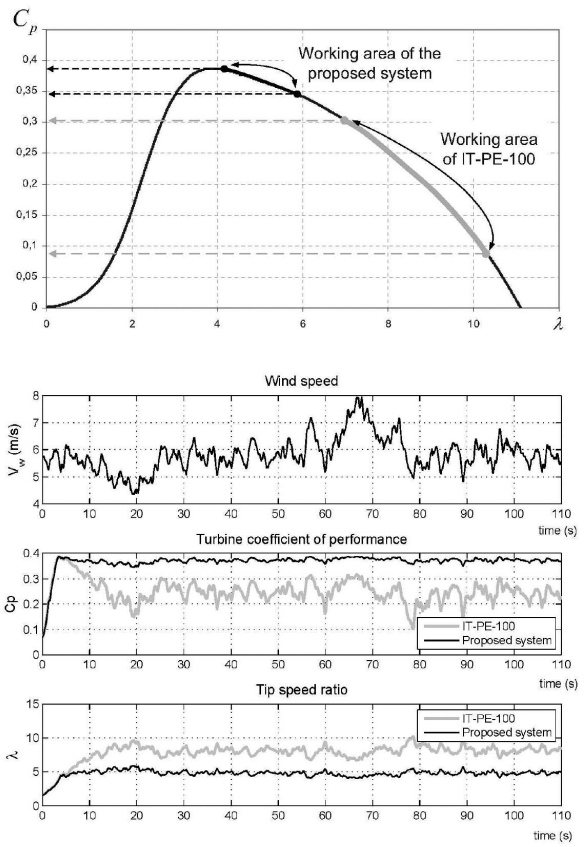

Fig. 13: System operation point in the C_p - λ curve and time variable response for a turbulent wind input

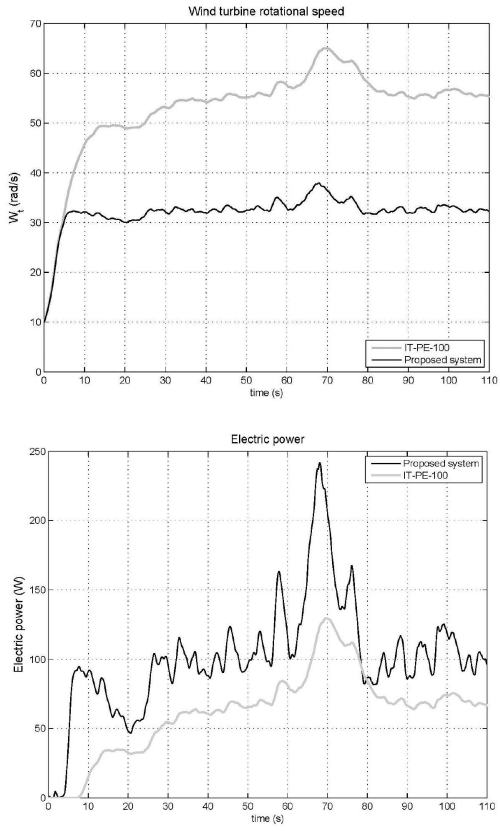

Fig. 14: Time variable response of rotational speed and power for a turbulent wind input

tion using a time series of wind with a turbulent flow had been done. It can be seen, in Fig. 13, that while the C_p in the controlled case remains to an approximate value of 0,37, on the uncontrolled case (IT-PE-100) almost does not exceed 0,3 and its average value is 0,24. With regard to the λ value in the controlled case the range vary from a minimum of 4,06 to a maximum of 5,89, which is close to the λ_{opt}. On the contrary the λ range of IT-PE-100 vary between 6,75 – 10,06. The Fig. 13 shows that while the C_p, in the controlled system, keeps a range of 0,3446-0,3865 the IT-PE-100 keeps very low turbine efficiency: C_p vary from 0,1021 to 0,3170.

Fig. 14 shows the evolution of the turbine rotational speed and the generated power in both cases. The speed in the controlled system is smaller than in the uncontrolled case. As to the generated power, it can be seen that the controlled system, with the DC/DC converter, transmits more power than the IT-PE-100 system. An increase of more than 38% in total energy converted to dc is predicted over the course of simulation.

Conclusion

One way of optimizing the power converting capabilities of a wind turbine is to run the turbine at its peak power coefficient. An algorithm was developed for this type of control using a variable speed turbine. The approaches done to model the system had been incorporated in Matlab and the simulations done indicate that the proposed simple open-loop control can offer significant advantages over a constant dc system. With this new system the rotational speed is reduced, which means that the items subject to rotating forces have less wear. Also, there is an improvement in the system efficiency; as a consequence there is an increase of the energy generated.

Acknowledgements

The work has been funded by the "Agència Catalana de Cooperació al Desenvolupament" (ACCD), the "Centre de Cooperació per al Desenvolupament" (CCD-UPC) and "Càtedra Alstom" from ETSEIB-UPC. The authors especially appreciate the cooperation and support given by "Soluciones Prácticas – Practical Action".

References

[1] J. A. Baroudi, V. Dinavahi, A. M. Knight: A review of power converter topologies for wind generators, IEEE International Conference on Electric Machines and Drives, 2005 15-18 May 2005 Page(s): 458 - 465

[2] Khan, M.S.; Iravani, M.R: Hybrid Control of a Grid-Interactive Wind Energy Conversion System, IEEE Transaction on Energy Conversion, Volume 23, Issue 3, Sept. 2008 Page(s):895 – 902

[3] Saiju, R.; Tamzarti, A.; Heier, S.: Performance Analysis of Small Wind Turbine Connected to a Grid through Modelling and Simulation, IECON 2007. 33rd Annual Conference of the IEEE Industrial Electronics Society, 2007. 5-8 Nov. 2007 Page(s): 1127 - 1131

[4] Driesen, J.; De Brabandere, K.; D'hulst, R.; Belmans, R.: Small wind turbines in the built environment: opportunities and grid-connection issues, Power Engineering Society General Meeting, 2005. IEEE 12-16 June 2005 Page(s):1948 - 1949 Vol. 2

[5] OECD/IEA. World Energy Outlook 2004.Chapter 10: Energy and Development (2004)

[6] John Byrne, Aiming Zhou, Bo Shen1, Kristen Hughes: Evaluating the potential of small-scale renewable energy options to meet rural livelihoods needs: A GIS- and lifecycle cost-based assessment of Western China's options", Energy Policy 35 (2007) 4391–4401

[7] Borowy, B.S.; Salameh, Z.M.: Dynamic response of a stand-alone wind energy conversion system with battery energy storage to a wind gust, IEEE Transaction on Energy Conversion, Volume 12, Issue 1, March 1997 Page(s): 73 -78

[8] Muljadi, E.; Drouilhet, S.; Holz, R.; Gevorgian, V: Analysis of permanent magnet generator for wind power battery charging, Thirty-First IAS Annual Meeting, IAS '96., Conference Record of the 1996 IEEE on Industry Applications Conference, 1996. Volume 1, 6-10 Oct. 1996 Page(s):541 - 548 vol.1

[9] De Broe, A.M.; Drouilhet, S.; Gevorgian, V: A peak power tracker for small wind turbines in battery charging applications, IEEE Transaction on Energy Conversion, Volume 14, Issue 4, Dec. 1999 Page(s):1630 - 1635

[10] Drouilnet, S; Muljadi, E; Holz, R; Gevorgian, V: Optimizing Small Wind Turbine Performance in Battery Charging Applications; National Renewable Energy Laboratory (NRL), May 1995

[11] Rodrigo, F.M.; de Lucas, L.C.H.; de Pablo Gomez, S.; de la Fuente, J.M.G.: Analysis of the Efficiency Improvement in Small Wind Turbines when Speed Is Controlled, IEEE International Symposium on Industrial Electronics, 2007. ISIE 2007. 4-7 June 2007 page(s): 437 - 442

[12] Chiroque, José: Microaerogenerador IT-PE-100 para electrificación rural, Soluciones practices ITDG, Serie Manuales nº 34

[13] Chiroque, José; Sánchez, Teodoro; Dávila, Celso: Microaerogeneradores de 100 y 500 W: Modelos IT-PE 100 y SP-500, Soluciones prácticas ITDG

[14] Jacek F. Gieras; Rong-Jie Wang; Maarten J. Kamper: Axial Flux Permanent Magnet Brushless Machines, 2004 Kluwer Academic Publishers, pp. 153 - 188

[15] NWTC Design Codes (AeroDyn by Dr. David J. Laino). http://wind.nrel.gov/designcodes/ Last modified 05-July-2005

[16] Z. M. Salameh, M. A. Casacca, and W. A. Lynch: A mathematical model for lead-acid batteries, IEEE Trans. Energy Convers., vol. 7, no. 1, pp. 93–98, Mar. 1992.

[17] M. Undeland T. P. Robbins W. Mohan, N. Power Electronics: Converters, Applications and Design, chapter 5. Line-frequency diode rectifers: line-frequency ac, uncontrolled dc, pages 79-120. John Wiley and Sons, INC., 1976

[18] A. M. Knight and G.E. Peters: Simple wind energy controller for an expanded operating range, IEEE Transaction on Energy Conversion, 20: 459-466, 2005.

[19] J. Velasquez: Mapa eólico preliminar del perú, Empresa de Administración de Infraestructura Eléctrica S.A., Lima-2007

The authors

Alba Colet-Subirachs received the Industrial Engineering degree from the school of Industrial Engineering of Barcelona (ETSEIB), Technical University of Catalonia (UPC), Barcelona, Spain, in 2009.. She worked at the Centre of Technological Innovation in Static Converters and Drives (CITCEA-UPC) in a cooperation project in which she got the experience in programming DSP applied to the power electronics converters. She is currently involved in Smart Electrical Grid projects at the Catalonia Institute for Energy Research (IREC). Her research interests include renewable energy integration in power systems and power electronics.

Oriol Gomis-Bellmunt received the degree in industrial engineering from the School of Industrial Engineering of Barcelona (ETSEIB), Technical University of Catalonia (UPC), Barcelona, Spain, in 2001 and the PhD in electrical engineering from the UPC in 2007. In 1999 he

joined Engitrol S.L. where he worked as project engineer in the automation and control industry. In 2003 he developed part of his PhD thesis in the DLR (German Aerospace center) in Braunschweig (Germany). Since 2004 he is with the Electrical Engineering Department of the UPC where he is lecturer and participates in the CITCEA-UPC research group. Since 2009 he is also with the Catalonia Institute for Energy Research (IREC). His research interests include the fields linked with smart actuators, electrical machines, power electronics, renewable energy integration in power systems, industrial automation and engineering education.

Daniel Clos received the degree in industrial engineering from the School of Industrial Engineering of Barcelona (ETSEIB), Technical University of Catalonia (UPC), Barcelona, Spain, in 1991. He is an associate professor at UPC and member of the Mechanical Engineering Department (DEM) and the Research Group on Development Cooperation and Human Development (GRECDH). He has 17 years of experience on Multibody Dynamics Simulation and his actual research activity is focused on the development of simulation models to improve the design of microwind turbines.

Guillermo Martín-Segura is a PhD student at the Technical University of Catalonia (UPC). He received the degree in Industrial Engineering from the School of Industrial Engineering of Barcelona (ETSEIB-UPC) in 2007 and a research scholarship from the Catalan Government to develop the PhD in the same year. Working in in the Centre of Technological Innovation in Static Converters and Drives (CITCEA-UPC) since 2005, he also collaborates with the Research Group on Development Cooperation and Human Development (GRECDH-UPC). His research interests are those linked with power electronics and specially those related to renewable energies, induction heating and engineering education.

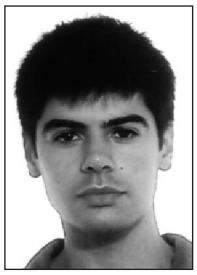

Adrià Junyent-Ferré received the Bs and Ms degrees in industrial engineering from the School of Industrial Engineering of Barcelona (ETSEIB), Technical University of Catalonia (UPC), Barcelona, in 2007 and the Ms degree in Automatic Control and Robotics from the UPC in 2009. He has been working on research projects as a grant student in the Electrical Engineering Department of the UPC since 2007. His research area of interest is the modeling and control of electrical machines and power converters and its use in wind generation systems.

Laia Ferrer-Martí is an associate professor at the Technical University of Catalonia (UPC). She has a degree in Industrial Engineering (1999) and holds a PhD from the UPC (2004). She develops her research activities at the Institute of Industrial and Control Engineering of the UPC and participates in the Research Group Development Cooperation and Human Development and in the Research Group Industrial Engineering and Logistics. Her research interests are focused on the development and application of quantitative techniques to solve industrial engineering problems: rural electrification, transportation routes, warehouse design, logistics systems, among others.

Roberto Villafáfila-Robles (S'05) was born in Barcelona, Spain, and received the degree in Industrial Engineering from the School of Industrial Engineering of Barcelona (ETSEIB), Universitat Politècnica de Catalunya (UPC), Spain, in 2005, and the PhD in Electrical Engineering from the UPC in 2009. Since 2003 he participates in the Centre of Technological Innovation in Static Converters and Drives (CITCEA) at UPC, where he is involved in technology transfer with the local industry due to research and innovation projects in the field of power quality, renewable energies and power systems. In 2006 he developed part of his PhD thesis at the Institute of Energy Technology, Aalborg University, Denmark. Since 2007 he is assistant professor in the Electrical Engineering Department of UPC at the Escola Universitària d'Enginyeria Tècnica Industrial de Barcelona (EUETIB). His research interests include power systems, distributed generation, integration of renewable energy into the networks and power quality.